Beyond Wide-Angle Images: Unsupervised Video Portrait Correction via Spatiotemporal Diffusion Adaptation

Wenbo Nie, Lang Nie, Chunyu Lin,* Jingwen Chen, Ke Xing, Jiyuan Wang, Yao Zhao
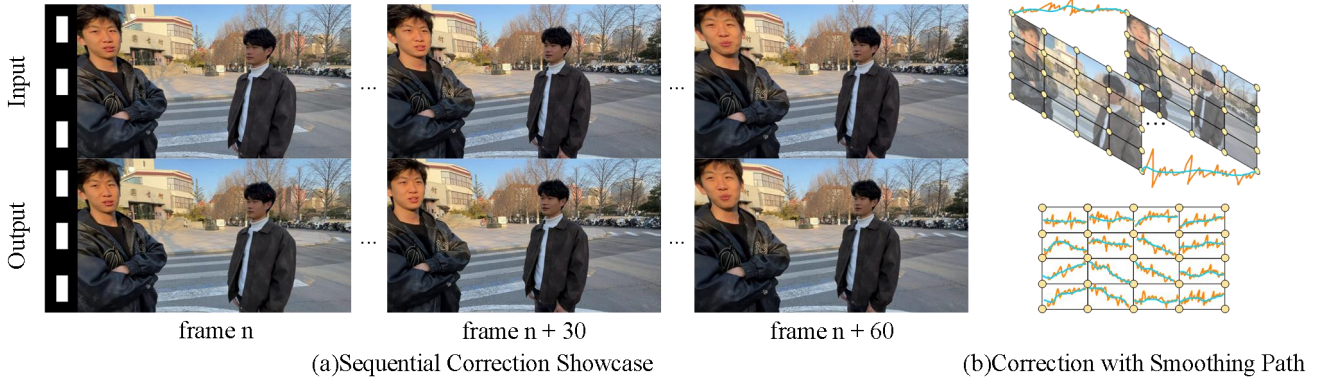
Figure 1. Our wide-angle video portrait correction results. (a) The first row shows a wide-angle phone video with edge distortion, corrected in the second row using our method while preserving spatiotemporal consistency. (b) Video correction introduces temporal shake (orange line in the figure), while our method smooths the trajectory (blue line).

Abstract

*Wide-angle cameras, despite their popularity for content creation, suffer from distortion-induced facial stretching—especially at the edge of the lens—which degrades visual appeal. To address this issue, we propose an image portrait correction framework using diffusion models named **ImagePD**. It integrates the long-range awareness of transformer and multi-step denoising of diffusion models into a unified framework, achieving global structural robustness and local detail refinement. Besides, considering the high cost of obtaining video labels, we then repurpose ImagePD for unlabeled wide-angle videos (termed **VideoPD**), by spatiotemporal diffusion adaption with spatial consistency and temporal smoothness constraints. For the former, we encourage the denoised image to approximate pseudo labels following the wide-angle distortion distribution pattern, while for the latter, we derive rectification trajectories with backward optical flows and smooth them. Compared with ImagePD, VideoPD maintains high-quality facial corrections in space and mitigates the potential temporal shakes sequentially. Finally, to establish an evaluation benchmark and train the framework, we establish a video portrait dataset with a large diversity in people number, lighting conditions, and background. Experiments demonstrate that the proposed methods outperform existing solutions quantitatively and qualitatively, contributing to high-fidelity wide-angle videos with stable and natural portraits. The codes and dataset will be available.*

1. Introduction

With the development of the self-media and videography industries, wide-angle lenses have become increasingly favored for the capability of capturing expansive scenes. However, such lenses inevitably introduce geometric distortions, particularly pronounced at the lens boundaries, resulting in background straight line curvatures and facial feature deformations in still images and video recordings.

Traditional wide-angle portrait correction methods typically require precise camera parameters (*e.g.*, focal length [29]) as a prerequisite, followed by stereographic projection, face and line detection, and energy optimization to achieve geometric correction [29]. Such a pipeline is complex in process and inapplicable when the relevant camera parameters are unknown. The same goes for video portrait correction work [17]. In contrast, learning-based solutions eliminate this issue [33] by directly learning the spatial mapping from wide-angle images to rectification flows in a supervised manner. However, these methods often exhibit noticeable temporal shakes when applied to videos. Moreover, there is currently a lack of datasets for video portrait

correction due to the significantly higher cost of labeling video data.

To this end, we take a pioneering step in achieving video portrait correction with diffusion models. First of all, we present a global-to-local portrait correction diffusion model, named **ImagePD**, to generate high-quality rectification flows, which integrates the advantages of both Transformer and diffusion models. The Transformer model establishes long-range geometric dependencies by capturing spatial global features across entire images, providing structural guidance for the subsequent diffusion process. The diffusion model refines high-fidelity flow patterns through iterative denoising guided by Transformer-derived structural information. This co-design enables structure-to-detail pixel-wise correction, where structural priors from the Transformer and detail-generation capacity from the diffusion model are synergistically combined.

More importantly, we propose an unsupervised spatiotemporal diffusion adaption approach to enable ImagePD the capability to rectify video sequences stably. The repurposed model, which we term **VideoPD**, addresses the issue of temporal shakes without requiring video correction labels. Concretely, we first use the pre-trained ImagePD to generate rectification flows for each video frame as pseudo-labels. When ImagePD is adapted to unseen wide-angle videos, these pseudo-labels can guide the denoising process, ensuring spatial consistency in facial corrections with the wide-angle distortion distribution prior. To enforce temporal smoothness, we derive rectification trajectories across sequential frames using backward optical flows and design a temporal smoothness constraint to mitigate sequential jitters. By unsupervised spatiotemporal adaptation with diffusion models, VideoPD achieves stable wide-angle video correction that not only preserves high-fidelity facial details but also frees from labor-intensive video annotations.

To establish an evaluation benchmark and train the proposed video portrait correction model, we construct a wide-angle video dataset with a wide diversity in scene, camera, and number of people. Finally, we conduct extensive experiments about portrait correction in both image and video, demonstrating our superiority over other solutions. The contributions center around:

- We propose the first portrait correction diffusion model, named **ImagePD**, which integrates long-range dependences of transformer and iterative refinements of diffusion models for global-to-local rectification.
- We design an unsupervised spatiotemporal diffusion adaption framework to transfer **ImagePD** to **VideoPD** without labeled videos. It combines spatio-temporal optical flows to track correction trajectories, establishing spatial consistency and temporal smoothness constraints.
- We present a video portrait dataset with wide-angle cameras and conduct extensive experiments to validate our

superior performance over existing solutions.

2. Related Work

2.1. Portrait Correction

Portrait correction in wide-angle images is a significant research area. Traditional methods, such as Shih et al.[29]'s content-aware warping, adjust distortions by analyzing image content and camera parameters. However, these methods bbnnv nbrely on camera parameters or complex inputs and are difficult to extend to video processing. Stereographic projection methods[29] can preserve local conformality but struggle with temporal consistency in videos.

Deep learning has introduced calibration-free solutions. Tan et al.[33] proposed a two-stage neural network leveraging wide-angle images and correction flow datasets. In contrast, Zhu et al. [47] developed a semi-supervised Transformer to reduce annotation costs. Nie et al.'s method CoupledTPS[23], iteratively couples limited TPS models with a warping flow to precisely correct facial features.

Portrait correction in wide-angle videos has garnered less research focus than image-based studies. Current deep learning methods, designed solely for static image processing, do not accommodate the temporal dynamics inherent in video data. This stems from the high cost of manually annotating wide-angle videos, which demands frame-by-frame effort and proves impractical for continuous video tasks, resulting in a scarcity of comprehensive training datasets.

Lai et al.[17]. introduced temporal consistency energy minimization based on traditional spherical projection and energy minimization to optimize videos. However, this method lacks a connection between the global information of wide-angle videos and the detailed information needed for facial correction. It also lacks adaptability and stability when dealing with complex environments and conditions.

To address this issue, we propose learning video correction principles from image networks.

2.2. Video stabilization

Traditional video stabilization techniques primarily stabilize the video by smoothing the feature trajectories between multiple frames or adjacent frames [18, 28, 35]. Subsequently, grid-based methods [20, 22, 35] and optical flow (Liu et al.[21]; Geo et al.[15]) have also been applied to represent motion, becoming key tools for stabilizing videos. With the rapid development of deep learning, deep learning methods have been applied to video stabilization technology [25, 39, 43, 45, 46], where the original video frames are input, and stabilized video frames are directly output. For example, Wang et al. [34] proposed an end-to-end learning framework, and Xu et al. [37] used adversarial networks to generate target images.DUT [38], which learns video

stabilization by simply watching unstable videos. Additional methods, including unsupervised online video stitching (Nie et al.[24]), and meta-learning-based approaches to improve full-frame stabilization (Ali et al.[1]), have been explored to enhance stability. These approaches, ranging from optical flow to deep learning models, provide valuable solutions for addressing video temporal shake in video portrait correction.

2.3. Diffusion Models

Diffusion models (DMs)[40] have recently achieved remarkable success in generative tasks, extending from image generation to video-related applications. In video generation, early advancements include Video Diffusion Models (VDM)[13], which adapted the 2D U-Net architecture from image DMs to a 3D U-Net for generating coherent video frames. To enhance temporal resolution, Ho et al.[12] introduced a cascade of video super-resolution models, improving the quality of generated sequences. Additionally, methods like Make-A-Video [30] achieved text-to-video generation by leveraging pre-trained text-to-image DMs, avoiding the need for paired text-video data.

More recent work focuses on video editing and enhancing temporal consistency. For example, Tune-A-Video [36] fine-tunes models on single input videos to produce coherent video outputs, while FateZero [26] ensures temporal consistency using attention-based blending techniques. Similarly, Rerender-A-Video [41] and VideoControlNet[14] introduce pixel-aware latent fusion and motion-aware adjustments to maintain visual consistency during edits.

3. Methodology

3.1. Overview

The overview of our method is shown in Fig. 2, where our framework operates in two cascaded stages: **correction** and **stabilization**.In the first stage, ImagePD tackles the distorted image I_s, producing precise optical flows using a Transformer-guided diffusion approach. The refined optical flow is then applied to generate a geometrically aligned image $\hat{I}_s$.

In the second stage, temporal pixel trajectories T are extracted from shaky video sequences, represented as the unstable video frames V_s. Using the corrected frames $\hat{I}_s$ as the reference, the final corrected and stabilized output V_{final} is computed as:

$$V_{\text{final}} = C(V_s \mid \hat{I}_s, T), \tag{1}$$

where C denotes the spatiotemporal fusion module.

3.2. ImagePD

As illustrated in Fig. 2(a,b), our ImagePD is a framework for high-quality portrait correction by predicting pre-cise optical flow fields to rectify facial distortions.

3.2.1. Model Architecture

In the first stage of ImagePD, we focus on capturing the global geometric structure of the distorted input image I_s. The Transformer network [47], denoted as MS-Unet in Fig. 2(a), with its advantage in capturing long-range information, extracts a set of intermediate layer features h that effectively reflect the global geometric structure of the distorted input image. These features h serve as a structural prior, guiding the diffusion model in the next stage to accurately align the facial geometry while preserving spatial coherence.

Building on the global structure from the first stage, this stage, as shown in Fig. 2(b), fines local details using a diffusion-based approach.

In order to ensure that the correction process primarily focuses on the area of the face, we use InsightFace [2, 3, 5–11, 27] as a pre-trained model to process the original facial image I_s, allowing accurate face detection and keypoint localization. Based on these detection results, a binary mask M is generated, which clearly delineates the facial region. This mask provides spatial guidance for subsequent processing and improves the quality of the correction. Leveraging the detail-handling capability of diffusion models, we form the conditioning input for ImagePD by concatenating M, I_s, and h:

$$x_{in} = cat[M, I_s, h] \tag{2}$$

Our approach leverages the iterative refinement capabilities of Denoising Diffusion Implicit Models (DDIM)[31], enabling iterative data generation through noise-adding and denoising processes. In DDIM, an original sample x_0 is gradually corrupted with Gaussian noise over T timesteps, eventually approximating a standard Gaussian distribution $x_T \sim \mathcal{N}(0, I)$. The reverse process starts from x_T and iteratively removes noise to recover a clean sample, modeled as a learned denoising transition.

A time-conditioned U-Net, denoted as ϵ_θ, is trained to predict the noise ϵ added at each step. During training, noise is added to x_0 to generate intermediate states x_t, and the model optimizes the following mean squared error (MSE) loss:

$$L = \mathbb{E}_{t \sim U(1,T),\, x_0 \sim q(x_0),\, \epsilon \sim \mathcal{N}(0,I)} \left[\|\epsilon - \epsilon_\theta(x_t, t)\|^2 \right] \tag{3}$$

Adapting this concept, ImagePD redefines the diffusion process to operate directly on optical flow fields.

The task of the diffusion network at this stage is not to directly generate the corrected facial image, but to predict an optical flow field F^{corr}. Compared to directly generating an image, the optical flow field offers sub-pixel precision, enabling more fine-grained guidance and correction of minor deformations in the image.
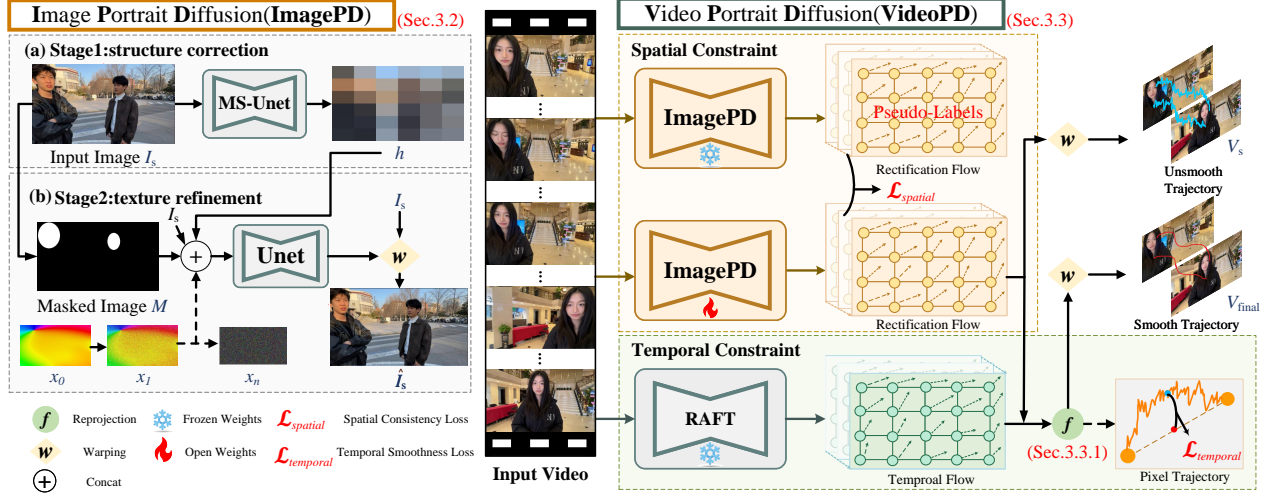
Figure 2. An overview of the proposed framework for portrait distortion correction, integrating Transformer networks and diffusion models. The framework consists of two stages: ImagePD for generating high-quality rectification flow and VideoPD for applying this correction to videos, ensuring spatiotemporal consistency and smooth stabilization.

By iteratively refining the predicted optical flow using the diffusion model, our method ultimately produces a highly accurate optical flow prediction. This prediction is then used to warp distortion correction on the facial image, producing the corrected output:

$$\hat{I}_s = \mathcal{W}(F^{corr}, I_s) \tag{4}$$

The warping operation $\mathcal{W}$ realigns the pixels in I_s according to the predicted flow, resulting in a natural facial appearance.

3.2.2. Optimization Objective

The model is optimized using a comprehensive loss function:

$$\mathcal{L}_{image} = \lambda_1 \mathcal{L}_{mask} + \lambda_2 \mathcal{L}_{photo} + \lambda_3 \mathcal{L}_{flow} \tag{5}$$

where $\mathcal{L}_{flow}$ ensures optical flow accuracy, $\mathcal{L}_{photo}$ enforces image quality, and $\mathcal{L}_{mask}$ enhances facial edge details, with λ_1, λ_2, and λ_3 as weighting coefficients.

Training objective: $\mathcal{L}_{image}$ comprises three components, each addressing a specific aspect of the correction process.

Optical Flow Loss $\mathcal{L}_{flow}$: Measures the difference between the model-predicted optical flow and the ground truth optical flow.

$$\mathcal{L}_{flow} = \frac{1}{HW} \sum_{h=1}^{H} \sum_{w=1}^{W} W \left(F^{Corr}(h, w) - F_{\text{gt}}(h, w) \right)^2 \tag{6}$$

Image Loss $\mathcal{L}_{photo}$: Evaluates the difference between the corrected image after optical flow correction and the ground

truth image.

$$\mathcal{L}_{photo} = \frac{1}{HW} \sum_{h=1}^{H} \sum_{w=1}^{W} W \left(\hat{I}_s(h, w) - I_{\text{gt}}(h, w) \right)^2 \tag{7}$$

Mask-based Sobel Loss $\mathcal{L}_{mask}$: Uses the Sobel operator to extract edge information and calculates the edge loss within the facial region mask.

$$\mathcal{L}_{mask} = \big[\left| G_x(F^{Corr}) - G_x(F_{\text{gt}}) \right| \\ + \left| G_y(F^{Corr}) - G_y(F_{\text{gt}}) \right| \big] \cdot M \tag{8}$$

3.3. VideoPD

Videos are dynamic sequences composed of continuous multi-frame images $\mathcal{I} = \{\mathcal{I}_1, \mathcal{I}_2, \ldots, \mathcal{I}_n\}$. To achieve unsupervised wide-angle video correction, we use pre-trained ImagePD to generate corrected optical flow for each frame as pseudo-labels. However, directly applying these pseudo-labels to the video frame sequence for correction results in severe temporal shakes sequentially, significantly decreasing the video's quality and visual experience. To address this issue, we propose further fine-tuning of ImagePD to enhance its adaptability in distortion video scenarios by introducing VideoPD.

3.3.1. Correction Trajectory

Our method aims to modulate and control the motion between corresponding frames, so we first use the RAFT [44] network to estimate the inter-frame optical flow from the original wide-angle video. For each pair of consecutive frames I_t and I_{t+1}, RAFT computes the backward optical flow $f_{t \to t+1}$ to avoid generating invalid regions. Next, each

The input at the t-th frame　　The input at the (t+1)-th frame

Flow t→t+1

Flow t+1→t

Corrected Backward Flow (t)　　Corrected Backward Flow (t+1)

Corrected Motion

The same location

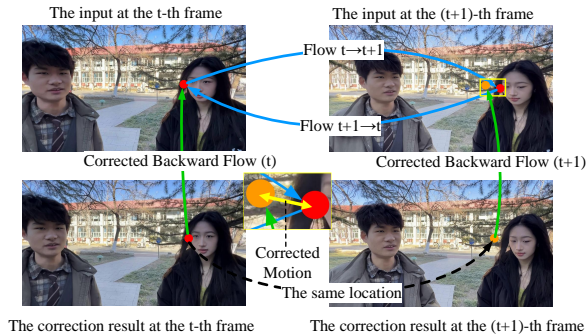The correction result at the t-th frame　　The correction result at the (t+1)-th frame

Figure 3. Illustration of the computation of $r(t + 1)$ in Eq. 9, depicting the integration of RAFT optical flow $f_{t \to t+1}$, corrected mesh G, and correction flows F_t^{Corr} and F_{t+1}^{Corr} for temporal stabilization.

frame is processed by the ImagePD module, which leverages a diffusion model to predict the optical flow of correction F_t^{corr}, effectively serving as a pseudo-label. This flow contains detailed adjustment information for the facial regions, addressing distortions introduced by the wide-angle lens.

To address the temporal shake caused by independent corrections between frames, we construct a series of two-dimensional meshes for each frame on the original frames. The pseudo-label optical flow F_t^{corr} is then used to adjust the positions of the control points in the mesh and we can obtain an updated mesh G.

To ensure smooth corrections across time, the corrected mesh G is used for reprojection onto the optical flow $f_{t \to t+1}$ from RAFT and the pseudo-label flow F_t^{corr}. This fusion yields a refined temporal optical flow F_t^{final}, which effectively mitigates warping shakes and ensures consistency between frames. A visual representation of this relationship Eq. 9 is provided in Fig. 3.

$$r(t + 1) = f_{t \to t+1}\Big(G + F_t^{\text{Corr}}\Big) + F_t^{\text{Corr}} - F_{t+1}^{\text{Corr}} \quad (9)$$

It can be further concatenated in temporal order from the initial moment to obtain the position at each moment as follows:

$$R(t) = r(1) + r(2) + \cdots + r(t) \quad (10)$$

where $r(1)$ is defined as a zero matrix. The rectified motion trajectory can be obtained by sequentially concatenating $R(1), R(2), \ldots, R(t), \ldots, R(N)$ over time. We achieve smooth trajectory stabilization and resolve video shaking issues by controlling the incremental stability of this pixel-level dense trajectory.

3.3.2. Spatiotemporal consistency

To achieve unsupervised video correction, we design our objective function $\mathcal{L}_{video}$ concerning two aspects: spa-

tial consistency and temporal smoothness.

$$\mathcal{L}_{video} = \mathcal{L}_{spatial} + \lambda \mathcal{L}_{temporal} \quad (11)$$

For the temporal smoothness, we use the previously derived video warping motion trajectories to achieve this functionality, constraining the video trajectories obtained from the domain-adapted ImagePD model to be as smooth as possible. For three consecutive frames, we encourage the trajectory position of the middle frame to lie between the trajectory positions of the preceding and following frames:

$$\mathcal{L}_{temporal} = \|R(t + 1) + R(t - 1) - 2R(t)\| \quad (12)$$

For spatial consistency, we leverage the pre-trained ImagePD model to ensure the quality of facial distortion correction within each frame. This is achieved by incorporating pseudo-labels generated by ImagePD, supervising the optical flow loss $\mathcal{L}_{flow}$ (Eq. 6) and the mask-based Sobel loss $\mathcal{L}_{mask}$(Eq. 8). These components maintain the structural integrity and edge details of the facial regions across individual frames, adapting the spatial correction capabilities from the image domain to the video domain.

3.4. Data preparation

Due to the lack of publicly available wide-angle video portrait datasets, we introduce a new dataset containing 136 clips, each with a resolution of 1080p at 30fps, ranging from 5 seconds to 90 seconds in duration(totaling 43,903 frames). The clips were captured using the iPhone 13 Pro, Gopro Hero 7, Samsung Galaxy S24, and Oneplus ace 2v, covering a wide variety of scenarios such as campuses, parks, shopping malls, classrooms, and other everyday settings. These clips encompass diverse scenarios, including content captured by self-media creators and film clips extracted from cinematic works. The number of people appearing in each scene varies from 1 to 6, reflecting diverse human dynamics. To enhance the dataset's diversity, we've also included footage shot in special conditions like nighttime environments. To authentically replicate real-world recording conditions, we deliberately introduced artificial shaking to simulate the instability inherent in handheld video capture. This design choice poses significant challenges for stabilization algorithms. Fig. 4 presents some examples of our wide-angle video portrait dataset.

4. Experiments

4.1. Dataset and Implement Details

Our methodology builds upon two core datasets: the established wide-angle image dataset [33] and our newly captured video dataset.

Image Data: In our experiments, we use the dataset from Tan et al.[33], which consists of 5133 training images and 129 test images captured with five wide-angle smartphones.

Video Data: For both training and testing phases, we utilized the dataset described in Sec. 3.4. The training set comprised 16 video sequences (7,134 frames) that comprehensively represent diverse capture devices, environmental conditions, and scene types, ensuring the model training across varied scenarios.

Training Process of ImagePD: Our framework employs a two-stage training protocol. In the first stage, we utilize the Adam optimizer[16] with an initial learning rate of 1×10^{-4}, training the model for 200 epochs. The subsequent texture refinement stage leverages high-dimensional features extracted from the initial phase. This feature, combined with image I_s and mask M, acts as the conditional guidance for the diffusion model to enhance fine-grained texture details. This stage implements a learning rate of 2×10^{-4}, with optimization conducted over 500,000 iterations.

Training Process of VideoPD: For VideoPD, we finetune the ImagePD model to maintain correction efficacy while smoothing temporal jitter. Training employs the Adam optimizer[16] with a learning rate of 2×10^{-4} over 300,000 iterations. The entire training process is conducted on a **single RTX 4090**.

4.2. Evaluation Metrics

Following Tan et al.'s work [33], we evaluate geometric correction performance using two established metrics: **LineAcc** quantifies how well straight edges retain geometric integrity by computing deviations between local slopes and the ideal global orientation. **ShapeAcc** assesses shape preservation via cosine similarity between reference and corrected landmarks, where higher values indicate better alignment. We also employ Jin et al.'s **Stability Score** (Avg, Trans, Rot)[4], which uses homography and FFT, to measure VideoPD's shake reduction, with higher scores denoting smoother videos.

4.3. Comparisons.

We evaluate our approach against existing methods across image and video modalities, providing comprehensive quantitative and qualitative results.

Image Comparisons. As shown in Table 1, our ImagePD achieves the second-best performance across LineAcc and ShapeAcc metrics, surpassed only by DualPriors[42]. This shows that our image correction model can retain the geometric integrity of straight edges

Method	Reference	LineAcc	ShapeAcc
Shih et al.[29]	TOG2019	66.143	97.253
Tan et al.[33]	CVPR2021	66.784	97.490
Zhu et al.[47]	CVPR2022	66.825	97.491
MOWA[19]	arXiv 2024	-	97.475
DualPriors[42]	ECCV2024	67.304	99.012
CoupledTPS[23]	TPAMI2024	66.808	97.500
ImagePD (Ours)	-	66.898	97.508

Table 1. Quantitative comparison of the proposed ImgaePD and different portrait correction methods.Higher LineAcc and ShapeAcc indicate better straight-line and face correction performance, respectively.

and preserve facial shape well. Furthermore, in the qualitative comparison presented in Fig. 5, we can further observe that ImagePD outperforms DualPriors[42] in the aforementioned aspects. This undoubtedly demonstrates that, despite DualPriors[42] achieving state-of-the-art performance on certain metrics, their approach exhibits noticeable abrupt artifacts at stitching boundaries and inconsistent head-to-body proportions in the images. This may be attributed to their method relying on a parallel network that separately rectifies the background and portrait before stitching them into a single image, with blank areas repaired using LaMa[32]. In contrast, Fig. 5(c) clearly illustrates that our method generates more natural and refined character appearances, highlighting the superiority of ImagePD.

Video Comparisons. In the video domain, our approach not only corrects individual frames but also prioritizes inter-frame continuity to mitigate severe visual jitter. As demonstrated in Table 2, VideoPD exhibits superior performance in handling rotational distortions while maintaining optimal stability. In Fig. 6, the red arrows and boxes highlight the unnatural or failed corrections in previous methods when processing video sequences, and these errors typically result in video discontinuity and poor visual perception. In contrast, our framework effectively corrects distortions while preserving the spatiotemporal consistency across the entire video sequence, underscoring the superiority of VideoPD. Additional video results can be found in the supplementary materials.

Method	Average	Translational	Rotational
CoupledTPS[23]	0.9811	0.9785	0.9836
DualPriors[42]	0.9477	0.9290	0.9664
VideoPD(Ours)	0.9886	0.9821	0.9951

Table 2. Quantitative Stability Metrics (Translation/Rotation) for Video Stabilization Models.

Notably, the impressive performance of our proposed method **ImagePD** and **VideoPD** is primarily attributed to

Figure 4. Our wide-angle video face dataset encompasses a broad range of scenes and showcases significant diversity in individuals. We present some examples from our dataset.

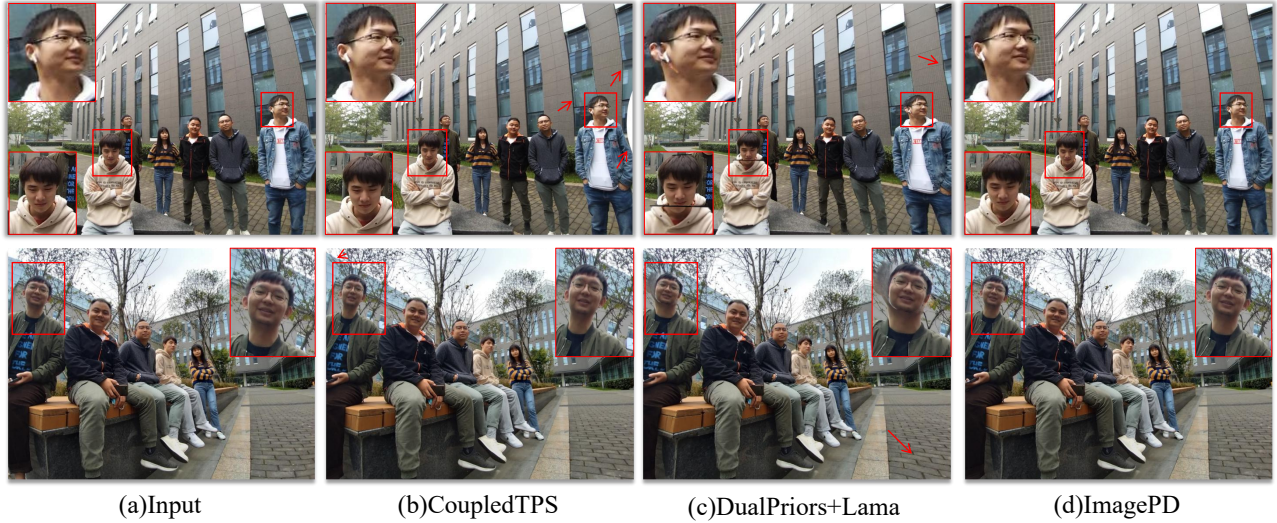| (a)Input	(b)CoupledTPS	(c)DualPriors+Lama	(d)ImagePD

Figure 5. Comparison of ImagePD with existing methods on wide-angle distorted images. ImagePD achieves superior restoration of natural facial features and reduced edge distortions compared to state-of-the-art alternatives.

the two-stage structural design. This framework combines the transformer's capacity for long-range dependency modeling with the diffusion model's multi-step denoising process, achieving global structural consistency and local refinement. By integrating these complementary mechanisms within a unified architecture, our approach achieves remarkable generation quality while maintaining spatial-temporal consistency across various distortion scenarios.

4.4. Ablation studies

In order to demonstrate the effectiveness of our approach and verify the impact of different components, we conducted a series of ablation experiments. In particular, we focus on different diffusion conditions, collaborative architecture design, and video correction trajectories.

Impact of Co-Designed Architecture and Conditional Guidance. Specifically, to independently analyze the impact of each component on correction quality, we designed four ablation scenarios: 1) Transformer Only: The Transformer predicts optical flow without diffusion, testing

its global structure modeling. 2)Diffusion with Condition (I_s): The diffusion model exclusively uses the distorted image I_s to predict optical flow, assessing its baseline detail correction. 3) Diffusion with Condition (I_s, M): A mask is applied that marks the face region in the distorted wide-angle image, serving as the conditioning input to guide the model's generation process. 4) Transformer + Diffusion with Condition (I_s, M): The Transformer provides a feature vector h concatenated with I_s and M to guide the diffusion model, evaluating their combined structural and detail refinement capabilities.

Transformer	Diffusion	M	I_s	LineAcc	ShapeAcc
✓				66.617	95.533
	✓		✓	66.249	97.465
	✓	✓	✓	66.687	97.488
✓	✓	✓	✓	66.898	97.508

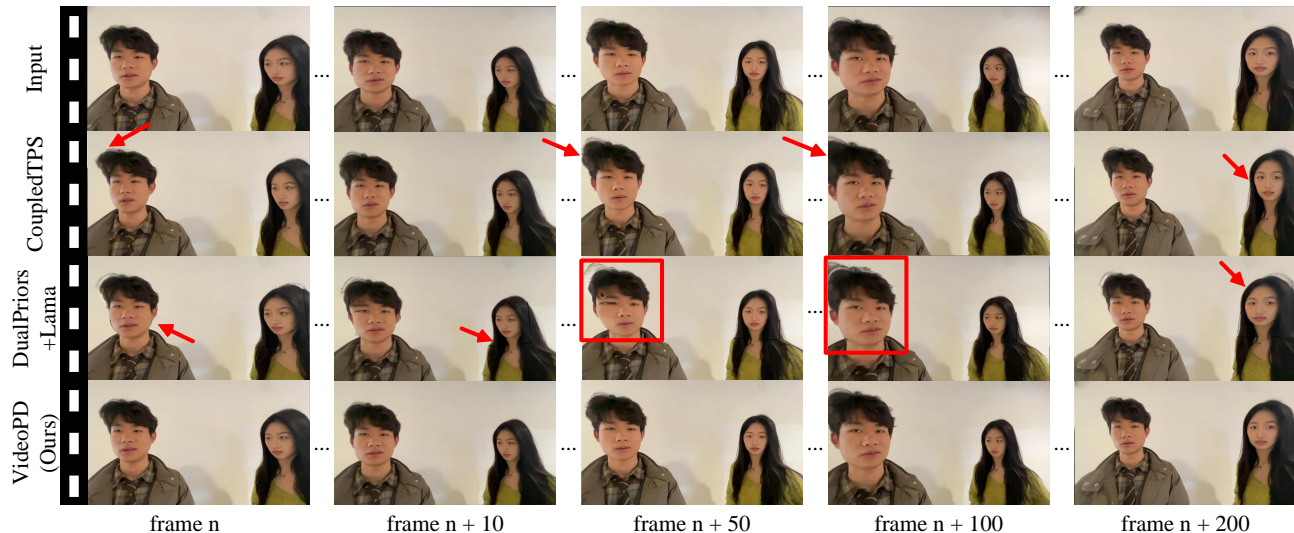Table 3. Ablations on the structure of co-designed architecture and different conditions.

Figure 6. Comparison with Existing Portrait Correction Methods in Wide-Angle Videos.

Table 3 presents the experimental results, clearly demonstrating the impact of each module. Specifically, when the Transformer model is integrated with the diffusion model, the scores of LineAcc and ShapeAcc achieve their peak values. These findings confirm our hypothesis that the joint transformer-diffusion architecture can significantly improve the performance of wide-angle lens distortion correction. Furthermore, the progressive incorporation of conditioning information highlights how each component contributes to the robustness and accuracy of portrait stability.

Method	Stability	LineAcc	ShapeACC
ImagePD	0.9325	66.898	97.508
VideoPD	0.9886	66.692	97.480

Table 4. Ablation Experiments Comparing ImagePD and VideoPD on Video Stabilization and Correction.

Impact of Spatiotemporal Smoothing on Video Correction. Our VideoPD model is a fine-tuned extension of the ImagePD model, specifically designed to address the challenges of video correction. Meanwhile, as mentioned before, the key difference between video and photo correction is the spatiotemporal consistency. Therefore, in this section, we directly compare the video results generated by VideoPD and ImagePD to evaluate whether VideoPD alleviates the warping shake caused by the correction process.

In fact, to mitigate the video shaking , some of the original correction of ImagePD will inevitably be compromised. In our experiments, we strive to balance correction and smoothing. This balance ensures that while we reduce the warping shake, we do not sacrifice too

much of the correction accuracy. Tab. 4 presents the results. ImagePD achieves excellent correction accuracy, while VideoPD, with spatiotemporal smoothing, increases Stability to 0.9886 (a 6.0% improvement), significantly reducing jitter. The minor decrease in Line/ShapeACC is statistically insignificant ($p > 0.05$, t-test), indicating that VideoPD effectively balances correction accuracy and interframe smoothness.

For further video results and more detailed analysis, readers can refer to the supplementary materials.

5. Conclusion

In this work, we introduce a novel approach to address facial distortion correction in both images and videos, marking the first application of diffusion models in the domain of portrait distortion correction. Our method represents the first deep learning-based solution for wide-angle video portrait correction, offering a significant advancement over traditional approaches. By leveraging image-level labels to learn the task of unlabeled wide-angle video correction, we drastically reduce the annotation burden and costs. Additionally, our proposed unsupervised framework, VideoPD, enhances spatiotemporal consistency while maintaining a smooth balance between correction and stabilization. We validate our method using a newly created wide-angle video dataset, demonstrating superior performance compared to existing approaches, showcasing its potential for wide-scale, automated, and accurate correction of wide-angle portrait distortion in still images and dynamic video sequences.

References

[1] Muhammad Kashif Ali, Eun Woo Im, Dongjin Kim, and Tae Hyun Kim. Harnessing meta-learning for improving full-frame video stabilization, 2024. 3

[2] Xiang An, Xuhan Zhu, Yuan Gao, Yang Xiao, Yongle Zhao, Ziyong Feng, Lan Wu, Bin Qin, Ming Zhang, Debing Zhang, and Ying Fu. Partial fc: Training 10 million identities on a single machine. In *ICCVW*, 2021. 3

[3] Xiang An, Jiangkang Deng, Jia Guo, Ziyong Feng, Xuhan Zhu, Yang Jing, and Liu Tongliang. Killing two birds with one stone: Efficient and robust training of face recognition cnns by partial fc. In *CVPR*, 2022. 3

[4] Jinsoo Choi and In So Kweon. Deep iterative frame interpolation for full-frame video stabilization. *ACM Transactions on Graphics*, 39(1), 2020. 6

[5] Jiankang Deng, Anastasios Roussos, Grigorios Chrysos, Evangelos Ververas, Irene Kotsia, Jie Shen, and Stefanos Zafeiriou. The menpo benchmark for multi-pose 2d and 3d facial landmark localisation and tracking. *IJCV*, 2018. 3

[6] Jiankang Deng, Jia Guo, Xue Niannan, and Stefanos Zafeiriou. Arcface: Additive angular margin loss for deep face recognition. In *CVPR*, 2019.

[7] Jiankang Deng, Jia Guo, Tongliang Liu, Mingming Gong, and Stefanos Zafeiriou. Sub-center arcface: Boosting face recognition by large-scale noisy web faces. In *Proceedings of the IEEE Conference on European Conference on Computer Vision*, 2020.

[8] Jiankang Deng, Jia Guo, Evangelos Ververas, Irene Kotsia, and Stefanos Zafeiriou. Retinaface: Single-shot multi-level face localisation in the wild. In *CVPR*, 2020.

[9] Baris Gecer, Jiankang Deng, and Stefanos Zafeiriou. Ostec: One-shot texture completion. In *Proceedings of the IEEE/CVF Conference on Computer Vision and Pattern Recognition (CVPR)*, 2021.

[10] Jia Guo, Jiankang Deng, Niannan Xue, and Stefanos Zafeiriou. Stacked dense u-nets with dual transformers for robust face alignment. In *BMVC*, 2018.

[11] Jia Guo, Jiankang Deng, Alexandros Lattas, and Stefanos Zafeiriou. Sample and computation redistribution for efficient face detection. *arXiv preprint arXiv:2105.04714*, 2021. 3

[12] Jonathan Ho, William Chan, Chitwan Saharia, Jay Whang, Ruiqi Gao, Alexey Gritsenko, Diederik P. Kingma, Ben Poole, Mohammad Norouzi, David J. Fleet, and Tim Salimans. Imagen video: High definition video generation with diffusion models, 2022. 3

[13] Jonathan Ho, Tim Salimans, Alexey Gritsenko, William Chan, Mohammad Norouzi, and David J. Fleet. Video diffusion models, 2022. 3

[14] Zhihao Hu and Dong Xu. Videocontrolnet: A motion-guided video-to-video translation framework by using diffusion model with controlnet, 2023. 3

[15] Jerin Geo James, Devansh Jain, and Ajit Rajwade. Globalflownet: Video stabilization using deep distilled global motion estimates, 2022. 2

[16] Diederik P. Kingma and Jimmy Ba. Adam: A method for stochastic optimization, 2017. 6

[17] Wei-Sheng Lai, Yichang Shih, Chia-Kai Liang, and Ming-Hsuan Yang. Correcting face distortion in wide-angle videos. *IEEE Transactions on Image Processing*, 31:366–378, 2022. 1, 2

[18] Ken-Yi Lee, Yung-Yu Chuang, Bing-Yu Chen, and Ming Ouhyoung. Video stabilization using robust feature trajectories. In *2009 IEEE 12th International Conference on Computer Vision*, pages 1397–1404, 2009. 2

[19] Kang Liao, Zongsheng Yue, Zhonghua Wu, and Chen Change Loy. Mowa: Multiple-in-one image warping model, 2024. 6

[20] Shuaicheng Liu, Lu Yuan, Ping Tan, and Jian Sun. Bundled camera paths for video stabilization. *ACM Trans. Graph.*, 32 (4), 2013. 2

[21] Shuaicheng Liu, Lu Yuan, Ping Tan, and Jian Sun. Steadyflow: Spatially smooth optical flow for video stabilization. In *Proceedings of the IEEE Conference on Computer Vision and Pattern Recognition (CVPR)*, 2014. 2

[22] Shuaicheng Liu, Ping Tan, Lu Yuan, Jian Sun, and Bing Zeng. Meshflow: Minimum latency online video stabilization. In *European Conference on Computer Vision*, 2016. 2

[23] Lang Nie, Chunyu Lin, Kang Liao, Shuaicheng Liu, and Yao Zhao. Semi-supervised coupled thin-plate spline model for rotation correction and beyond. *IEEE Transactions on Pattern Analysis and Machine Intelligence*, 46(12):9192–9204, 2024. 2, 6

[24] Lang Nie, Chunyu Lin, Kang Liao, Yun Zhang, Shuaicheng Liu, Rui Ai, and Yao Zhao. Eliminating warping shakes for unsupervised online video stitching, 2024. 3

[25] Zhan Peng, Xinyi Ye, Weiyue Zhao, Tianqi Liu, Huiqiang Sun, Baopu Li, and Zhiguo Cao. 3d multi-frame fusion for video stabilization, 2024. 2

[26] Chenyang Qi, Xiaodong Cun, Yong Zhang, Chenyang Lei, Xintao Wang, Ying Shan, and Qifeng Chen. Fatezero: Fusing attentions for zero-shot text-based video editing, 2023. 3

[27] Xingyu Ren, Alexandros Lattas, Baris Gecer, Jiankang Deng, Chao Ma, and Xiaokang Yang. Facial geometric detail recovery via implicit representation. In *2023 IEEE 17th International Conference on Automatic Face and Gesture Recognition (FG)*, 2023. 3

[28] Ethan Rublee, Vincent Rabaud, Kurt Konolige, and Gary Bradski. Orb: An efficient alternative to sift or surf. In *2011 International Conference on Computer Vision*, pages 2564–2571, 2011. 2

[29] YiChang Shih, Wei-Sheng Lai, and Chia-Kai Liang. Distortion-free wide-angle portraits on camera phones. *ACM Trans. Graph.*, 38(4), 2019. 1, 2, 6

[30] Uriel Singer, Adam Polyak, Thomas Hayes, Xi Yin, Jie An, Songyang Zhang, Qiyuan Hu, Harry Yang, Oron Ashual, Oran Gafni, Devi Parikh, Sonal Gupta, and Yaniv Taigman. Make-a-video: Text-to-video generation without text-video data, 2022. 3

[31] Jiaming Song, Chenlin Meng, and Stefano Ermon. Denoising diffusion implicit models, 2022. 3

[32] Roman Suvorov, Elizaveta Logacheva, Anton Mashikhin, Anastasia Remizova, Arsenii Ashukha, Aleksei Silvestrov, Naejin Kong, Harshith Goka, Kiwoong Park, and Victor Lempitsky. Resolution-robust large mask inpainting with fourier convolutions. *arXiv preprint arXiv:2109.07161*, 2021. 6

[33] Jing Tan, Shan Zhao, Pengfei Xiong, Jiangyu Liu, Haoqiang Fan, and Shuaicheng Liu. Practical wide-angle portraits correction with deep structured models, 2021. 1, 2, 5, 6

[34] Miao Wang, Guo-Ye Yang, Jin-Kun Lin, Song-Hai Zhang, Ariel Shamir, Shao-Ping Lu, and Shi-Min Hu. Deep online video stabilization with multi-grid warping transformation learning. *IEEE Transactions on Image Processing*, 28(5): 2283–2292, 2019. 2

[35] Yu-Shuen Wang, Feng Liu, Pu-Sheng Hsu, and Tong-Yee Lee. Spatially and temporally optimized video stabilization. *IEEE Transactions on Visualization and Computer Graphics*, 19(8):1354–1361, 2013. 2

[36] Jay Zhangjie Wu, Yixiao Ge, Xintao Wang, Weixian Lei, Yuchao Gu, Yufei Shi, Wynne Hsu, Ying Shan, Xiaohu Qie, and Mike Zheng Shou. Tune-a-video: One-shot tuning of image diffusion models for text-to-video generation, 2023. 3

[37] Sen-Zhe Xu, Jun Hu, Miao Wang, Tai-Jiang Mu, and Shi-Min Hu. Deep video stabilization using adversarial networks. *Computer Graphics Forum*, 37(7):267–276, 2018. 2

[38] Yufei Xu, Jing Zhang, Stephen J. Maybank, and Dacheng Tao. Dut: Learning video stabilization by simply watching unstable videos. *IEEE Transactions on Image Processing*, 31:4306–4320, 2022. 2

[39] Junlan Yang, Dan Schonfeld, Chong Chen, and Magdi Mohamed. Online video stabilization based on particle filters. In *2006 International Conference on Image Processing*, pages 1545–1548, 2006. 2

[40] Ling Yang, Zhilong Zhang, Yang Song, Shenda Hong, Runsheng Xu, Yue Zhao, Wentao Zhang, Bin Cui, and Ming-Hsuan Yang. Diffusion models: A comprehensive survey of methods and applications, 2024. 3

[41] Shuai Yang, Yifan Zhou, Ziwei Liu, and Chen Change Loy. Rerender a video: Zero-shot text-guided video-to-video translation, 2023. 3

[42] Lan Yao, Chaofeng Chen, Xiaoming Li, Zifei Yan, and Wangmeng Zuo. Combining generative and geometry priors for wide-angle portrait correction, 2024. 6

[43] Jiyang Yu and Ravi Ramamoorthi. Robust video stabilization by optimization in cnn weight space. In *2019 IEEE/CVF Conference on Computer Vision and Pattern Recognition (CVPR)*, pages 3795–3803, 2019. 2

[44] Tianjun Zhang, Shishir G. Patil, Naman Jain, Sheng Shen, Matei Zaharia, Ion Stoica, and Joseph E. Gonzalez. Raft: Adapting language model to domain specific rag, 2024. 4

[45] Minda Zhao and Qiang Ling. Pwstablenet: Learning pixel-wise warping maps for video stabilization. *IEEE Transactions on Image Processing*, 29:3582–3595, 2020. 2

[46] Weiyue Zhao, Xin Li, Zhan Peng, Xianrui Luo, Xinyi Ye, Hao Lu, and Zhiguo Cao. Fast full-frame video stabilization with iterative optimization, 2023. 2

[47] Fushun Zhu, Shan Zhao, Peng Wang, Hao Wang, Hua Yan, and Shuaicheng Liu. Semi-supervised wide-angle portraits correction by multi-scale transformer, 2022. 2, 3, 6